Max-Planck-Institut
für Mathematik
in den Naturwissenschaften
Leipzig

An Atomistic to Continuum Model for Biopolymers Self-Assembled Aggregation

(revised version: August 2009)

by

Leonid Berlyand, Maxim V. Fedorov, and Lei Zhang

Preprint no.: 32 2009

AN ATOMISTIC TO CONTINUUM MODEL FOR BIOPOLYMERS SELF-ASSEMBLED AGGREGATION

Abstract. We want to address the following problem of hierarchical modeling of the structure of biopolymer self-assembly, and relate the marcoscale mechanical and geometrical property to their microscale molecular property, for example, how to link the chirality and the amphiphilicity of the single amino acid to the shape of their supramolecular aggregates, or mathematically, how to derive the elastic parameters from the parameters at the atomistic scale.

1. Biological Background: Self Assembly of Supramolecules

We model self-assembled aggregation of biomolecules, in particular we study peptide self-assembled systems, which may serve as a model system to study the aggregation process in amyloid disease. Peptides are short chain of biopolymers which are formed by amino acids linked head-to-tail with covalent peptide bonds.

The self-assembly mechanism is: single peptides in solution can undergo a conformational change from random coil to β strands and assemble side by side to form tapes resembling β sheets. With increasing concentration, more complex "amyloid-like" structures such as ribbons (double tapes), fibrils, fibers can be developed. In this work, we will only study the self-assembled $\beta-$sheet tapes. The future goal will be the study of the hierarchical structure of self-assembled system.

Experiments reveal that there is substantial structural similarity between the fibrils formed by β-peptide self-assembly and the amyloid fibrils found in conformational diseases such as Huntington's, Alzheimer's and type-II diabetes.

A peptide bond is a covalent bond that is formed between two adjacent amino acids when the carboxyl group of one amino acid reacts with the amino group of another amino acids. Atoms can be modeled as imaginary hard spheres with the radius defined as *van der Waals radius*. From the fact that each atom within a molecule occupies a certain amount of space, which is assocaited to the energy cost due to overlapping electron clouds (Pauli or Born repulsion), and this may affect the molecule's preferred shape (conformation) and reactivity, in particular this requirement limits greatly the possible bond angles in a polypeptide chain. This constraint and other steric interactions severely restrict the variety of three-dimensional possible arrangements of atoms (or conformations). In the following, we will see how to mathematically model these *bonded interactions* on the atomistic scale.

The conformation of supramolecule is, however, further constrained by many different sets of weak noncovalent bonds (or *nonbonded interactions*) that form between atoms which are not linked by covalent bonds, in different peptide chains or in different parts of a single peptide chain. The weak bonds are mainly of four types: hydrogen bonds, ionic bonds, van der Waals attractions, and hydrophobic/hydrophilic interaction. Individual noncolvalent bonds are 30-300 times weaker than the typical covalent bonds that create biological molecules [1]. But many weak bonds can act in parallel to hold two peptide chain or two regions of a peptide chain tightly together. The stability of each folded shape is therefore determined by the combined strength of large numbers of such noncovalent bonds.

2. Mathematical Background: Multiscale Methods, Coarse Graining, Homogenization, etc

Physical problems with many scales are ubiquitous in material sciences. To make them more accessible to analysis, it is often preferable to make the assumption of scale separation (with an explicit small parameter $\varepsilon \to 0$ and study an ε family of problems) and symmetry (periodicity, quasi-periodicity, or ergodicity). Essential progress has been made in this direction within the context of homogenization theory (Γ-, G- and H- convergence), to give a few examples out of a vast literature, let us refer to [7] (Bensoussan, Lions, and Papanicolaou) and [13] (Jikov, Kozlov, and Oleinik). Recently, these analytics approaches have been applied to study the discrete-to-continuum limits for thin elastic films [21].

In real applications, we often need to compute the solution numerically. A direct simulation of the multiscale problem, which involves a wide range of spatial and time scales, is still difficult even with state-of-the-art supercomputers and algorithms. We have to resort to the so called **multiscale methods** to solve the problem on the coarser scale. More precisely, we need to know how to extract and transfer information from fine scales to coarse scales and how to use the obtained information to construct the coarse scale solver which is efficiently computable. In different context and literatures, this procedure can be referred to as *numerical homogenization* or *numerical upscaling* or *coarse graining*.

For example, the Multi-scale Finite Element Method (MsFEM) of Hou and Wu [12] has been a large source of inspiration in numerical algorithms (particularly for reservoir modeling in geophysics). Furthermore, E and Engquist et al. have developed a general framework of the heterogeneous multi-scale methods [23] (HMM) and applied the method to complex fluids, solids, stochastic ODE and many other applications.

Including MsFEM and HMM, most multi-scale methods are based on solving local cell problems. Some approaches, like HMM, use the cell problem to calculate effective media properties, then solve an effective equation on the coarse scale. A detailed review of this kind of upscaling methods can also be found in [9]. Other methods, like MsFEM, incorporate the fine scale features of the problems into basis elements. The coupling of small scales with coarse scales is then performed through a numerical formulation of the global problem using these multi-scale basis. In most cases, these methods can only be justified in one-dimensional case, in the case of periodic or ergodic media with scale separation, or when the solution is sufficiently smooth.

However, in many practical situations, it may not be possible to distinguish finitely many well separated scales (e.g., different lengths of oscillations), and one has to deal with a medium (rather than a sequence of media) that has no periodicity or ergodicity property. It is then heuristic to apply methods based on local cell problems to solve problems with non-separable scales and often leads to qualitatively incorrect results.

Furthermore, in most problems in material sciences, one has to deal with a given medium and not with an ε family of media. In particular, for our problem, it is not possible to find a small parameter characterizing the medium with respect to which one could perform an asymptotic analysis.

For partial differential equations with nonseperable scales, early results on this last level of difficulty can be traced back to the work of Osborn and Babuska [3, 4] in which a change of coordinates is introduced in one dimensional and quasi-one dimensional divergence form elliptic problems, allowing for efficient dimensional approximations. The analysis of homogenization of scalar divergence form elliptic, parabolic and hyperbolic equations with arbitrarily complex coefficients that in addition satisfies Cordes type condition in arbitrary dimensions has been performed

in a series of papers by H. Owhadi and L. Zhang [19, 18, 20] using global harmonic coordinates as a change of coordinates. While in two dimensions the Cordes type condition does not impose any restrictions on the coefficients, in dimensions three and higher it restricts the anisotropy of the tensor a(x). In the paper of L. Berlyand and H. Owhadi [8] analogous homogenization approximation is obtained without imposing the Cordes-type condition. For vectorial problems (e.g., elasticity) the change of coordinates can not be used. However, the approach of [8] does not rely on any coordinate change and therefore it allows one to treat both scalar and vectorial problems in a unified framework.

2.1. **Mathematical Modeling of Supramolecular Tapes.** The emergence of nanotechnology has drawn tremendous interest in the mathematical and numerical study of molecular tapes and membranes, in particular for graphene monolayers and for self-assembled membranes. At the fine scale, the system is governed by atomistic potentials, and the geometry of tape is determined by the position of atoms and moieties. At the coarse scale, usually it can be described in continuum mechanics as an elastic tape with thickness zero. The problem of deriving continuum description from atomistic potential has been previously studied by several authors, Friesecke and James [10] proposed a scheme to construct continuum models directly from atomistic models for thin film and nono-rods. Arroyo and Belyschko [2] proposed the exponential Cauchy-Born rule for crystalline sheets. In [25] Yang and E showed an alternative approach for , a generalization of Cauchy-Born rule with consideration of curvature effect. In these models, nonlinear elasticity are proposed as the continuum behaviour of the system. However, since all these models are strongly nonlinear and its evaluation requires the inner displacement relaxation and the membrane and bending contributions are tightly coupled.

On the other hand, in the simplest case, when the conformation of the membrane is axisymmetric, the deformation energy functional of a membrane can be decomposed as twisting, bending and splay mode. For example, in the work of Ref. [6], a simple coarse grained model is used. Assume that the length of the tape and the width are constant (fluctuations in the inter-peptide distance and in the single peptide end-end distance are in fact negligible if compared to the ones related to twist and bend). Therefore, the splay deformation is negligible and only twisting and bending energy are considered.

However, this model has limited accuracy because it is based on the axisymmetric configuration and the isotropicity assumption. As a trade off, we will use a model which permits general configuration, and also has satisfied accuracy when the deformation is not so large.

Analogous to the Kirchhoff-Saint Venant model of finite elasticity, the simplest isotropic model for a two-dimensional continuum elastic energy can be split into membrane energy and bending energy, and is of the form [2]

$$W_{approx} = W_m + W_b = \frac{1}{2}[2\mu E : E + \lambda(\text{tr } E)^2] + \frac{1}{2}[a(2H)^2 + bK] \tag{1}$$

where λ and μ are the 2D Lamé coefficients, E is the Green strain tensor, the mean curvature H and the Gaussian curvature K are the invariants of the curvature tensor, and a and b are bending elastic moduli. Since $\int_\Omega K dx$ is a topological invariant of the surface by Gauss-Bonnet theorem, the term involving K can be treated as a topological constant in the strain energy density.

In recent work of [14], the authors are deriving bending constant from an atomistic model for graphene monolayer. If the equilibrium configuration is known, a formula of the bending modulus can be derived analytically from the knowledge of atomistic potential, if only the bond length potential, bond angle potential and dihedral angle potential are considered. Any potential with

only the nearest neighbor interactions would lead to zero bending modulus of the monolayer, which is nonphysical.

If the elastic sheet is inextensible, the in-plane contribution to the potential energy is negligible. If the equilibrium configuration of the elastic sheet is not flat, namely there is a spontaneous curvature H_0, the elastic energy can be furture simplified to

$$W = \frac{1}{2}[a(H - H_0)^2 + bK + c] \tag{2}$$

Note this is the celebrated Helfrich energy functional.

3. Problem and Method

For the continuum modeling of the self-assembled tape, we use molecular dynamics at the fine scale and extract parameters of the coarse grained model from the fine scale simulation. Results of atomistic simulations and continuum simulations will be compared to justify our model.

3.1. **Setup of the Problem.** We consider the following molecular system: $M = 60$ $\beta-$peptides are placed into a planar, parallel arrangement which forms a flat tape. A single amino acid is represented by three beads (two for the backbone and one for the side chain). The bead denoted as X stands for the moiety $C_\alpha H - C'O$ while Y represents the NH group on the backbone. The tape has two different sides: one "covered" by S_2 side chains and the other "covered" with S_1 side chains. Starting from this initial configuration, we run atomistic simulation to find the equilibrium configuration. The molecular systems are studied by varying both the chiral strength (CS) and the asymmetry (SAA) between the Lennard-Jones interaction for the pairs $S_2 - S_2$ and $S_1 - S1$, the parameters CS and SAA will be explained in the next section.

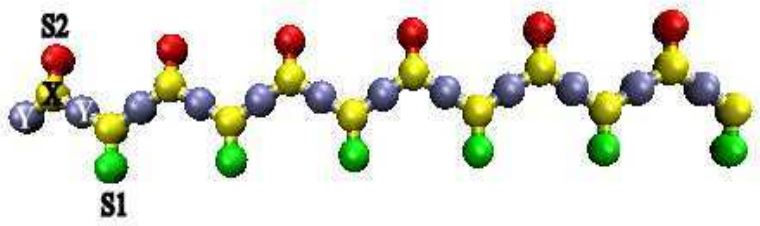

Figure 1. Geometry of the model peptide

3.2. **Molecular Dynamics at Atomistic Scale. Atomistic Scale Energy**

The atomistic scale potential energy is composed of the two types of components, bonded energy and nonbonded energy. We use a simplified atomic potential,

$$E_{atom} = \sum_{bonds} U_{bond} + \sum_{angles} U_{angle} + \sum_{dihedrals} U_{tors} + \sum_i \sum_{j \neq i} U_{LJ}(r_{ij}) \tag{3}$$

This model is well tested and now actively used for self-assembled aggregation of peptides, for example, see [6] and references therein. The parameters can reproduce results which coincide with experimental data. The numerical values of the bonded and nonbonded energy parameters used in our model somewhat correspond to the ones typically used in fully atomistic force fields.

Concerning the purely phenomenological parameters, such as the chirality-related parameters, their values were chosen to reproduce the experimental range of the macroscopic twist. The bonded energy consists of the following terms [6]

(1) bond length potential

$$U_{bond} = \frac{K_b}{2}(r - r_{eq})^2 \tag{4}$$

where $K_b = 200.0\text{Kcal/mol}\cdot\text{Å}^{-2}$ and $r_{eq} = 2.0\text{Å}$, the length of each bond is thus restrained towards the equilibrium value via the above harmonic potential.

(2) bond angle potential

$$U_{angle} = \frac{K_\theta}{2}(\theta - \theta_{eq})^2 \tag{5}$$

where $K_\theta = 40.0Kcal/mol$ and $\theta_{eq} = 120°$, $0°$ for angles centered at X and Y beads respectively. Bond angles defined via triplets $X_i - Y_{i+1} - X_{i+1}$, $Y_i - X_i - Y_{i+1}$, $Y_i - X_i - S1_i(S2_i)$ and $S1_i(S2_i) - X_i - Y_{i+1}$ are controlled by the above harmonic potential.

(3) dihedral angle potential

$$U_{tors} = D_{ijkl}\cos(3\alpha - \delta_{ijkl}) - G_{ijkl}\cos(\alpha - \delta_{ijkl}) \tag{6}$$

two angles shares a common bond form a dihedral, for every such set of 4 atoms, this potential is used to exclude overlap of the first atom and the last atom. In this model, $ijkl$ can be $YXYX$, $XYXY$, and $\delta ijkl = \pi$.

while Lennard-Jones potential is a simplified model for the nonbonded interaction energy

(1) Lennard-Jones potential

$$U_{LJ}(r) = 4\varepsilon[\big(\frac{\sigma}{r}\big)^{12} - \big(\frac{\sigma}{r}\big)^{6}] \tag{7}$$

is used to model non-bonded interaction,

We used the same Lennard-Jones functional form (with = 2.0 A) for reproducing the interactions between the side chain beads S_1 and S_2.

The bending of the β-sheet can be attributed to the following two physical origins at the molecular level,

(1) single strands in a β-sheet possess a right-handed twist along the backbone direction, this twist along the peptide backbone can be measured by the dihedral angle defined by the quadruplet $C_\beta(i) - C_\alpha(i) - C_\alpha(i+2) - C_\beta(i+2)$ where i refers to the i-th residue within the single strand. Single β-strands with such a rightChand helical nature assemble at a finite angle with respect to their neighbors and this angle transfers the chirality from the single strands (molecules) to the level of the mesoscopic assembly. $S2_iX_iX_{i+1}S1_{i+1}$ or $S1_jX_jX_{j+1}S2_{j+1}$.

three different values for the dihedral parameter δ_{ijkl}, namely 165°, 160° and 155° corresponding to systems with "chiral strength" $CS = 1, 2, 3$, respectively.

(2) the asymmetry due to different Lennard-Jones interaction strength of side group S_1 and S_2

the nonbonded asymmetry is realized by setting $\varepsilon_1 = 1.0kcal/mol$, and ε_2 parameter is taking the values in the set 1.0, 2.0, 3.0, 4.0, 5.0, 6.0, 7.0, 8.0, 9.0 (kcal/mol), which indexed by SAA=0,1,2,3,4,5,6,7,8

Indeed, since *in situ* we can easily change the asymmetry by, for example, changing the pH value of the solution by adding bases or acids.

A Lennard-Jones term involving only the backbone beads X and Y is used to model the intermolecular hydrogen bonding network typical of β-sheet structures: where $\varepsilon = 5.0$ kcal/mol, $\sigma = 2.0$ A for XX and YY pairs and $\sigma = 3.0$ A for XY pairs. We used the same LJ functional form (with $\sigma = 2.0$ A) for reproducing the interactions between the side chain beads (see more details below). The numerical values of the bonded and non.bonded energy parameters used in our model somewhat correspond to the ones typically used in fully atomistic force fields. Concerning the purely phenomenological parameters, such as the chirality related parameters ijkl, their values were chosen to reproduce the experimental range of the macroscopic twist.

In [14], the authors discussed the bending modulus for monolayer graphene, and identified the physical origin for the nonvanishing bending modulus as bond angle effect and dihedral angles.

3.3. **Bending and Twist: Simple coarse grained elastic energy.** On the other hand, in the simplest case, the deformation energy functional of a membrane can be decomposed as twisting, bending and splay mode. For example, in the work of Ref. [6], a simple coarse grained model is used. Assume that the length of the tape and the width are constant (fluctuations in the inter-peptide distance and in the single peptide end-end distance are in fact negligible if compared to the ones related to twist and bend). Therefore, the splay deformation is negligible and only twisting and bending energy are considered.

The coarse grained elastic energy of the tape can be characterized by twist and bending. It is derived in [16, 6] under the assumption that the configuration of the tape is axisymmetric,

$$E_{el} = K_{bend}(\Theta_b - \Theta_{b0})^2 + K_{twist}(k - k_0)^2 \tag{8}$$

k is the pitch wave number (twist angle), which is the measure of the chirality of the tape. Θ_b is the curvature angle, which is a measure of bending. Both k and Θ_b can be calculated using atomistic positions.

Pitch wave number (twist angle) as a measure of the chirality of the tapes. The pitch wave number k is calculated by taking the vector $x_{ij} = (X_2^i - X_1^j 1)$, where X_1^i is the position of monomer X in the lth residue within the ith strand. The use of the vector x_{ii} is justified because the molecules behave themselves essentially as rigid rods. In more details,

$$k_{i,i+1} = acos(\frac{x_{ii}}{\|x_{ii}\|} \cdot \frac{x_{i+1,i+1}}{\|x_{i+1,i+1}\|}) \tag{9}$$

The calculation of the parameter k, which is related to a cosine, misses the correct sign. To overcome this, we first define

$$\begin{aligned} r_{12} &= x_{ii} \\ r_{32} &= x_{i,i+1} \\ r_{34} &= x_{i+1,i+1} \end{aligned} \tag{10}$$

second, we calculate the sign of k is as sign$(r_{12} \cdot r_{32} \times r_{43})$. Monitoring the sign of this quantity gives information about the handedness of the helical cluster.

Curvature angle

In addition, we calculate the angle Θ_b, as a measure of the curvature (bending) of the tape. From the formula, $c = 2(s/\Theta_b)\sin(\Theta_b/2)$. Using the approximation

$$\sin(x) \simeq x - (x^3)/3! \tag{11}$$

with the chord length defined as

$$c = \frac{1}{2M}\sum_{i=1}^{M} |Y_i(6) - Y_{i+2}(6)| + |Y_i(7) - Y_{i+2}(7)| \tag{12}$$

and with the arc length defined as

$$s = \frac{1}{2M}\sum_{i=1}^{M} |Y_i(6) - Y_{i+1}(6)| + |Y_{i+1}(6) - Y_{i+2}(6)| + |Y_i(7) - Y_{i+1}(7)| + |Y_{i+1}(7) - Y_{i+2}(7)| \quad (13)$$

where i is an index over the peptide position within the tape and the indexes 6 and 7 refer to the positions of the two central residues within the peptide molecule. We define the sign of Θ_b as positive when the bending is toward the S_2 side of the tape and negative when the bending is toward the S_1 side of the tape.

Elastic constants In the paper of Bellesia, Fedorov et al.[6], Langevin dynamics is used, K_{bend} and K_{twist} are estimated with the assumption that Θ_b and k are Gaussian distributed,

$$\begin{array}{l} K_{bend} = k_B T/(2\langle \Delta\Theta_b^2 \rangle) \\ K_{twist} = k_B T/(2\langle \Delta k^2 \rangle) \end{array} \quad (14)$$

3.4. **Curvature elasticity: a general continuum elasticity model.** To represent general shape of self-assembled tape, and accurately quantify the potential energy of the self-assembled system, we need more sophiscated elastic model. In this work, we use a linear elasticity model for elastic tape for a trade-off between accuracy and efficiency [2],

$$W_{approx} = W_m + W_b = \frac{1}{2}[2\mu E : E + \lambda(\text{tr } E)^2] + \frac{1}{2}[a(2H)^2 + bK] \quad (15)$$

where λ and μ are the 2D Lamé coefficients, E is the Green strain tensor, the mean curvature H and the Gaussian curvature K are the invariants of the curvature tensor, a and b are bending elastic moduli. Since $\int_\Omega K dx$ is a topological invariant of the surface by Gauss-Bonnet theorem, the term involving K can be treated as a topological constant in the strain energy density.

In [6], it is assumed that the length of the tape and the width are constants, namely, fluctuations in the inter-peptide distance and in the single peptide end-end distance are in fact negligible if compared to the ones related to twisting and bending. In the continuum case, this corresponds to the so called *isometric* deformations, i.e., significant deformations in bending but unnoticeable deformation in the membrane modes (shearing and stretching).

Although a complete treatment will consider the nonlinear coupling of bending and membrane energy, the composition of elastic energy into membrane and bending (flexural) energy is well known [22], for example, Ge et al. proposed a geometric argument that the stored energy of a continuous inextensible plate has the form $\int_\Omega c_H H^2 + c_K K dA$ for material coefficients c_H and c_K. In our case, the equilibrium configuration is not flat, but a curved surface, therefore, the deformation energy of the tape can be simplified from (1) to

$$E_{el} = \int_\Gamma a(x)(H - H_0)^2 dx + C \quad (16)$$

H_0 is the mean curvature of the equilibrium(reference) configuration, note that in our case, the reference configuration is not flat, therefore $H_0 \neq 0$ in general. This energy captures the essential geometric nonlinearity of the problem, the problem will be how to obtain the effective elastic constant $a(x)$ and calculate the mean curvature H and H_0 from discrete data. When $a(x)$ is homogeneous, we can use bending constant a

$$E_{el} = a\int_\Gamma (H - H_0)^2 dx + C \quad (17)$$

as shown in [14], the bending modulus

The shape of the tape is represented by the position of atoms. Since the flat configuration of the tape is a 60×12 rectangle lattice, we can divide each rectangle cell into two triangles by connecting northwest and southeast corners of the cell. In this way, we have a regular triangulation. To calculate the curvature for this triangulated 2 dimensional surface, we can use polynomial reconstruction (for example, splines) and analytical evaluation, however, this often leads to undesired behavior such as spurious oscillation[15]. On the other hand, piecewise linear triangle mesh can provide a simple and reliable approximation of the continuous surface which is suitable for our case. We can use the techniques which developed recently in computer graphics to calculate discrete curvatures, which is more natural and robust [15]. Namely, we can directly go from atomistic configuration to discretized problem, and do not need to use continuum description as an intermediate step.

Let S be a surface embedded in $\mathbb{R}^3$, for each point on the surface S, we can locally approximate the surface by its tangent plane, orthogonal to the normal vector $\mathbf{n}$. Local bending of the surface is therefore measured by *curvatures*. For every direction e_θ, the normal curvature $\kappa^N(\theta)$ is defined as the curvature of the curve that belongs to both surface S and the intersecting plane which contains $\mathbf{n}$ and e_θ.

3.5. **Notions from differential geometry.** Let S be a smooth surface in $\mathbb{R}^3$, suppose that H is the mean curvature of S and G is the Gaussian curvature of S. The two principal curvatures κ_1 and κ_2 of the surface S with their associated orthogonal directions e_1 and e_2 are extremum values of all the normal curvatures, which is the curvature of the curve of the normal section with the surface. The mean curvature H is defined as the average of normal curvature

$$H = \frac{1}{2\pi}\int_0^{2\pi} \kappa^N(\theta)d\theta = \frac{\kappa_1 + \kappa_2}{2} \tag{18}$$

The Gaussian curvature is defined as the product of the two principle curvatures:

$$G = \kappa_1\kappa_2 \tag{19}$$

These two curvatures represent important local properties of a surface. $H = 0$ is the Euler-Lagrange equation for surface area minimization, which provides a direct relation between surface area minimization and mean curvature flow:

$$2H\mathbf{n} = \lim_{diam(\mathcal{A})} \frac{\nabla\mathcal{A}}{\mathcal{A}} \tag{20}$$

where $\mathcal{A}$ is a infinitesimal area around a point P on the surface, $diam(\mathcal{A})$ its diameter, and ∇ is the gradient with respect to the (x, y, z) coordinates of P. We will denote by $\mathbf{K}$ the operator that maps a point P on the surface S to the vector $\mathbf{K}(P) = 2H(P)\mathbf{n}(P)$. $\mathbf{K}$ is also known as the Laplace-Beltrami operator for the surface S.

Gaussian curvature can also be expressed as a limit:

$$2H\mathbf{n} = \lim_{diam(\mathcal{A})} \frac{\mathcal{A}^{\mathcal{G}}}{\mathcal{A}} \tag{21}$$

where $\mathcal{A}^{\mathcal{G}}$ is the area of the image of the Gauss map associated with the infinitesimal surface $\mathcal{A}$.

3.5.1. *Discrete Curvature.* For the definition of discrete curvature, we will follow the line of [24, 11]. For a triangulated surface, the discrete curvatures – mean curvature, Gaussian curvature, principal curvatures and principal directions are deined on the vertices of the triangulation. 1-ring neighbors of a vertex are all the vertices which are connected to the vertex by one edge. The

discrete curvatures on a vertex are defined locally and only depend on the positions of the vertex itself and its 1-ring neighbors.

For a vertex on a triangulated surface, it is not staightforward to define quantities like tangent plane or normal vector as we can do for a smooth surface. Alternatively, one can define geometric quantities of the triangulated surface at a vertex as spatial averages around this vertex, and prove the consistency of the definition if the geometric quantity converges to the corresponding pointwise definition as the mesh is refined. For example, the mean curvature $\bar{H}$ at a vertex P is defined as

$$\bar{H} = \frac{1}{\mathcal{A}} \int_{\mathcal{A}} H dA \tag{22}$$

where $\mathcal{A}$ is a properly chosen area around P.

If all the triangles are non-obtuse, $\mathcal{A}$ can be chosen as the Voronoi cell around P (figure 2(b))

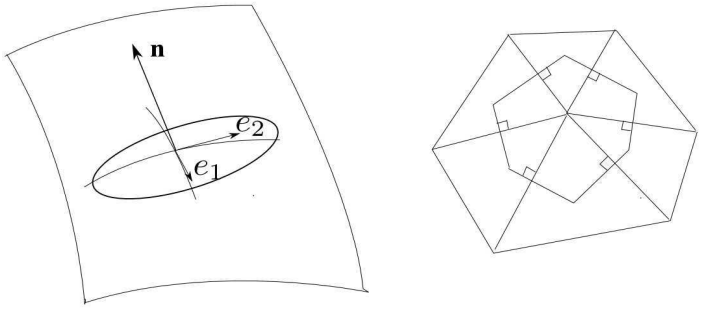

(a) ***Principal directions*** e_1 ***and*** e_2 ***associated with two principal curvatures*** κ_1 ***and*** κ_2

(b) ***Voronoi cell around a vertex which can be used to define discrete curvature***

FIGURE 2

The mean curvature normal operator can be expressed as the Laplace-Beltrami operator under conformal parameters u and v

$$\int_{\mathcal{A}} K(x) dA = -\int_{\mathcal{A}} \Delta_{u,v} x du dv \tag{23}$$

By Gauss's theorem, the area integral of the the Laplacian over a surface going through the midpoint of each 1-ring edge of a triangulated domain can be expressed as a function of the node values and the angles of the triangulation. The integral will thus reduces to the following form

$$\int_{\mathcal{A}} K(x) dA = \frac{1}{2} \sum_{j \in N_1(i)} (cot\alpha_{ij} + cot\beta_{ij})(\mathbf{x}_i - \mathbf{x}_j) \tag{24}$$

where α_{ij} and β_{ij} are the two angles opposite to the edge $(\mathbf{x}_i, \mathbf{x}_j)$, and $N_1(i)$ is the set of 1-ring neighbor vertices of vertex i.

Discretizing the tape by piecewise linear mesh, we express the discrete bending energy can therefore expressed as a summation over verticies

$$E_B = \sum_P (H(P) - H_0(P))^2 \text{area}(\mathcal{A}(P)) \tag{25}$$

In fact, the total energy can be represented as a sum of membrane and bending energy

$$E_{el} = E_M + k_B E_B \tag{26}$$

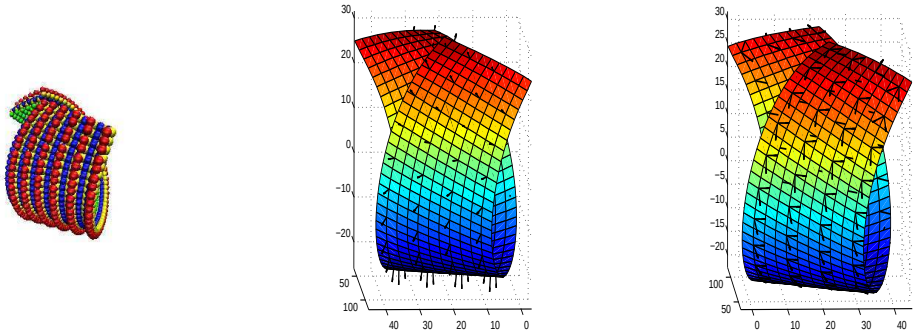

(a) ***Atomistic configuration with parameters W=5, CS=1*** (b) ***Mean curvature normal vector*** $\mathbf{K}(x)$ (c) ***Principal directions*** e_1 ***and*** e_2 ***associated with two principal curvatures*** κ_1 ***and*** κ_2

FIGURE 3

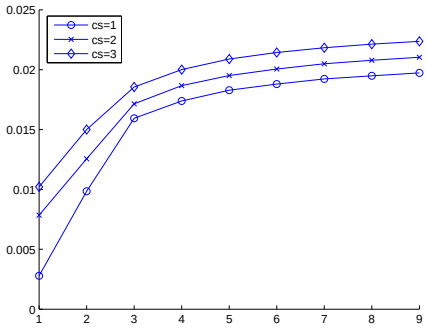

FIGURE 4. mean curvature for tapes with parameterscs=1,2,3, w=1,2,3,4,5,6,7,8,9

where k_B is the bending or flexural stiffness, and E_M is the membrane energy. We use $E_M = k_L E_L + K_A E_A$, where

$$E_L = \sum_e (1 - \|e\|/\|e_0\|)^2 \|e_0\| \tag{27}$$

a summation over edges, measures local change in length, while

$$E_A = \sum_A (1 - \|A\|/\|A_0\|)^2 \|A_0\| \tag{28}$$

a summation over areas of triangles, measures local change in area.

In the implementation, we usually use large k_L and k_A to approximately enforce the *isometric* constrain.

3.6. **Atomistic to Continuum by Energy Matching.** The main goal is to derive the continuum model from the atomistic model numerically. Our method is in the spirit of [19, 8, 17] and our ongoing work on mathematical analysis of atomistic to continuum method for general nonperiodic media. Note that in [5], Babuška and Sauter introduced the method of local energy matching for solving lattice equations. In [17], the energy matching method is used for numerical coarsening of inhomogeneous elastic materials. Namely, we enforce that the elastic energy of the continuum model (26) matches the total energy of the atomistic model (3) for all possible displacement fields; if the continuum model is inhomogeneous, we can subdivide the domain into

subdomains which the material parameters are homogenous, and enforce the equality within each subdomain,

$$E_{el} = E_{atom} \tag{29}$$

The displacement fields are computed by fine scale atomistic model. Therefore the best we can do is to satisfy the above equality by just a few displacements: if these test displacement fields can capture typical deformations, we will have achieved our goals.

The underlying mathematical assumption for the energy matching method to work will be the existence of a low dimensional approximating manifold to the potentially complicated high dimensional nonlinear atomistic system. This can be seen as a generalization of the celebrated Cauchy-Born rule or homogeneous deformation method. However, when the media is nonperiodic, or when the media is finite, the deformation is not homogeneous anymore, therefore, it is desirable to use the solutions of the whole problem instead of a cell problem. On the other hand, we only need to compute (29) finite times to solve for the effective coefficients, the nonlinearity is only geometric in (26).

Once we have the elastic energy of an atomistic tape, we can calculate boundary value problem for the tape on the continuum scale. Usually, we can do a minimization of the coarse grained continuum elastic energy with respect to boundary conditions as contains, and find the deformed configuration, which is much faster than atomistic simulation.

4. Numerical Experiments

To justify the numerical method, we will compare the results obtained by direct atomistic simulations with the results of the continuum elastic model.

The $M = 60$ peptides are placed into a planar parallel arrangement which forms a flat tape. We compute the equilibrium configuration first by using atomistic simulation, specifically, we minimize the potential energy at temperature $T = 0$. Once we have the equilibrium configuration, we can calculate the spontaneous curvature H_0 and bending constant. All the atomistic simulations are done by *NAMD*, and all the continuum simulation are done using *Matlab*, the optimization is done by BFGS linear search.

In the numerical experiments, we will consider three examples. First we consider the simple coarse grained model. In the second example, we fix the two shorter sides of the tape, then we use the obtained parameters to compute the deformed configuration using the elastic model, and compare it with the atomistic simulation. For the third example, we calculate the equilibrium configuration of the tape composed of $M = 120$ peptides using the elastic model.

4.1. **Simple coarse grain model.** In this case, it suffices to use two independent atomistic solutions to determine the elastic constants K_{bend} and K_{twist}. Substitute these two solutions into (29) we have two equations for K_{bend} and K_{twist}, solve the equations we obtain these elastic constants. Although the application to coarse grained model 8 is almost trivial, we would like to show that the elastic constants obtained by our method coincide with the elastic constants obtained in [6] at least in the order of magnitude.

We have some primary results for the case CS=1, SAA=5, and we see that K_{bend} and K_{twist} are of the same order as the result in [6].

4.2. **Tape with fixed sides.** In this example, we consider a deformed tape with two shorter sides fixed, by matching the energy, we can calculate that $k_b \simeq 2.5$, we also choose $k_L = k_A = 100 * k_b$ in order to approximately enforce the isometric condition,

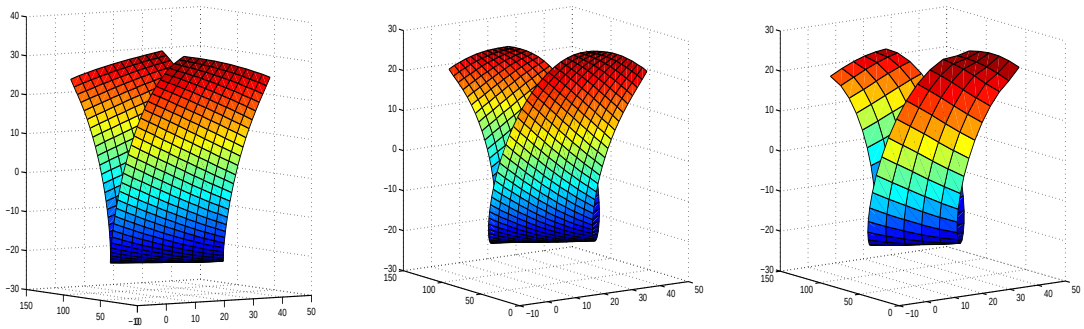

(a) ***reference configuration, MD simulation,*** [6] **(b)** ***deformed configuration with shorter sides fixed, MD computed by elastic model simulation*** **(c)** ***deformed configuration***

FIGURE 5. tape with fixed sides.

4.3. **Using obtained parameter to calculate longer molecular tape.** We can use the parameters computed for $M = 60$ peptides to calculate the equilibrium configuration for self-assembled system of $M = 120$ peptides.

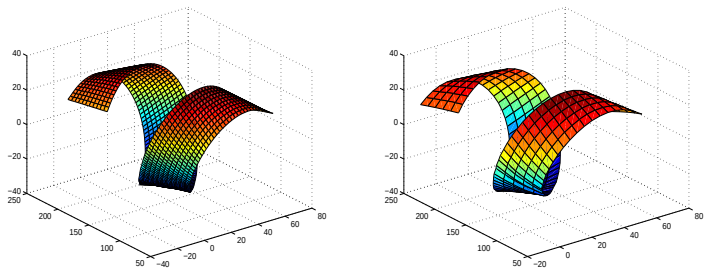

(a) ***equilibrium configuration by atomistic simulation, MD*** **(b)** ***equilibrium configuration by elastic model simulation***

FIGURE 6. tape of $M = 120$ peptides.

and mean curvature

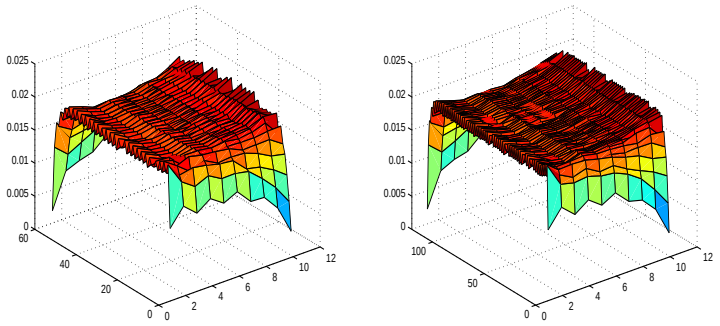

(a) *equilibrium configuration by atomistic simulation* **(b) *equilibrium configuration by elastic model***

FIGURE 7. tape of $M = 120$ peptides.

from the figures, we can see that the mean curvature is almost constant in the interior of the tape; the drop of the mean curvature at the boundaries is related with the finite size of the system and should be negligible for systems with large size.

5. Conclusion

In this work, we obtain curvature elasticity model from atomistic model by energy matching method numerically, the curvature elasticity is expressed geometrically on a piecewise linear triangle mesh. Numerical experiments show that qualitatively satisfiable results can be obtained.

6. ACKNOWLEDGEMENTS

The work of Leonid Berlyand was partially supported by NSF grant DMS-0708324 and DOE grant DEFG02-08ER25862.

References

[1] B. Alberts, A. Johnson, J. Lewis, M. Raff, K. Roberts, and P. Walter. *Molecular biology of the cell*. Garland Science, New York, 4th edition, 2002.

[2] M. Arroyo and T. Belytschko. Finite element methods for the non-linear mechanics of crystalline sheets and nanotubes. *International Journal for Numerical Methods in Engineering*, 59(3):419–456, 2003.

[3] I . Babuška, G . Caloz, and J .E. Osborn. Special finite element methods for a class of second order elliptic problems with rough coefficients. *SIAM J. Numer. Anal.*, 31(4):945–981, 1994.

[4] I. Babuška, G. Caloz, and J. E. Osborn. Generalized finite element methods: Their performance and their relation to mixed methods. *SIAM Journal on Numerical Analysis*, 20(3):510–536, 1983.

[5] I. Babuška and S.A. Sauter. Efficient solution of anisotropic lattice equations by the recovery method. *SIAM J. Scientific Computing*, 30(5):2386–2404, 2008.

[6] G. Bellesia, M. V. Fedorov, and E. G. Timoshenko. Structural transitions in model beta-sheet tapes. *The Journal of Chemical Physics*, 128(19):195105, 2008.

[7] A. Bensoussan, J. L. Lions, and G. Papanicolaou. *Asymptotic analysis for periodic structure*. North Holland, Amsterdam, 1978.

[8] L. Berlyand and H. Owhadi. A new approach to homogenization with arbitrarily rough coefficients for scalar and vectorial problems with localized and global pre-computing, 2009. (*available at http://arxiv.org/abs/0901.1463*).

[9] C. L. Farmer. Upscaling: A review. *Numerical Methods in Fluids*, 40:63–78, 2002.

[10] G. Friesecke and R. D. James. A scheme for the passage from atomic to continuum theory for thin films, nanotubes and nanorods. *Journal of the Mechanics and Physics of Solids*, 48:1519–1540, 2000.

[11] E. Grinspun, A. N. Hirani, M. Desbrun, and P. Schröder. Discrete shells. In *Proceedings of the 2003 ACM SIGGRAPH/Eurographics symposium on Computer animation*, pages 62–67. Symposium on Computer Animation, 2003.

[12] T. Y. Hou and X. H. Wu. A multiscale finite element method for elliptic problems in composite materials and porous media. *J. Comput. Phys.*, 134(1):169–189, 1997.

[13] V. V. Jikov, S. M. Kozlov, and O. A. Oleinik. *Homogenization of Differential Operators and Integral Functionals*. Springer-Verlag, 1991.

[14] Q. Lu, M. Arroyo, and R. Huang. Elastic bending modulus of monolayer graphene. *J. Phys. D: Appl. Phys.*, 42, 2009.

[15] M. Meyer, M. Desbrun, P. Schröder, and A.H. Barr. Discrete differential-geometry operators for triangulated 2-manifolds. In Hans-Christian Hege and Konrad Polthiers, editors, *Visualization and Mathematics III*, pages 35–57. Springer-Verlag, Heidelberg, 2003.

[16] I. A. Nyrkova, A. N. Semenov, A. Aggeli, and N. Boden. Fibirl stability in solutions of twisted beta-sheet peptides: a new kind of micellization in chiral systems. *The European Physical Journal B*, 17:481–497, 2000.

[17] H. Owhadi, L. Kharevych, P. Mullen, and M. Desbrun. Numerical coarsening of inhomogeneous elastic materials. *preprint*, 2009.

[18] H. Owhadi and L. Zhang. Homogenization of parabolic equations with a continuum of space and time scales. *SIAM Journal on Numerical Analysis*, 46(1):1–36, 2007.

[19] H. Owhadi and L. Zhang. Metric based upscaling. *Communications on Pure and Applied Mathematics*, 60(5):675–723, 2007. (*Preprint available at Arxiv, math.NA/0505223.*).

[20] H. Owhadi and L. Zhang. Homogenization of the acoustic wave equation with a continuum of scales. *Computer Methods in Applied Mechanics and Engineering*, 198(3–4):397–406, 2008.

[21] Bernd Schmidt. *Effective theories for thin elastic films*. PhD thesis, University of Leipzig, 2006.

[22] D. Terzopoulos, J. Platt, A. Barr, and K. Fleischer. Elastically deformable models. *Computer Graphics*, 21(4):205–214, 1987. Proc. ACM SIGGRAPH'87 Conference, Anaheim, CA, July, 1987.

[23] B. Engquist W. E, X. Li, W. Ren, and E. Vanden-Eijnden. The heterogeneous multiscale method: A review., 2004. (*Preprint, http://www.math.princeton.edu/multiscale/review.pdf*).

[24] M. Wardetzky, M. Bergou, D. Harmon, D. Zorin, and E. Grinspun. Discrete quadratic curvature energies. *Computer Aided Geometric Design*, 24(8–9):499–518, 2007.

[25] Z. Yang and W. E. Generalized cauchy-born rules for elastic deformation of sheets, plates, and rods: Derivation of continuum models from atomistic models. *Physical Review B*, 74(18):184110, 2006.